# Supplementary Information

## Developing stable organic radical anions to achieve long persistent luminescence for afterglow lighting

*Gaozhan Xie, Mingjian Zeng, Xin Zhang, Ansheng Luo, Jingru Zhang, Fei He, Xin Wang, Yang Hu, Weiguang Wang, Yannan Xie, Huanhuan Li, Runfeng Chen*, Ye Tao**

G. Xie, M. Zeng, X. Zhang, A. Luo, J. Zhang, F. He, X. Wang, Y. Hu, W. Wang, Y. Xie, H. Li, R. Chen, Y.Tao

State Key Laboratory of Organic Electronics and Information Displays & Institute of Advanced Materials (IAM), Jiangsu National Synergistic Innovation Center for Advanced Materials (SICAM), Nanjing University of Posts & Telecommunications, 9 Wenyuan Road, Nanjing 210023, China

E-mail: iamrfchen@njupt.edu.cn; iamytao@njupt.edu.cn

G. Xie

State Key Laboratory of Luminescent Materials and Devices and Institute of Polymer Optoelectronic Materials and Devices, South China University of Technology, Guangzhou 510640, Guangdong, China.

Y. Tao

Songshan Lake Materials Laboratory, Dongguan, Guangdong, 523808 China

**Content**

## 1. Synthesis and characterization

### Materials

The manipulations involving air-sensitive reagents were performed in an atmosphere of dry Argon (Ar). The chemicals and solvents, unless otherwise specified, were purchased from commercials and used without further purification.

### Measurements

$^{1}H$ and $^{13}C$-nuclear magnetic resonance (NMR) spectra were recorded on a Bruker Ultra Shield Plus 400 MHz instrument using $CDCl_3$ as the solvent and tetramethylsilane (TMS) as the internal standard. MALDI-TOF-MS was performed on Bruker autoflex speed MALDI-TOF instrument. High-performance liquid chromatogram (HPLC) spectra were collected by an Agilent 1100 spectrometry via monitoring the onset absorption at 346 nm.

### Synthesis and preparation

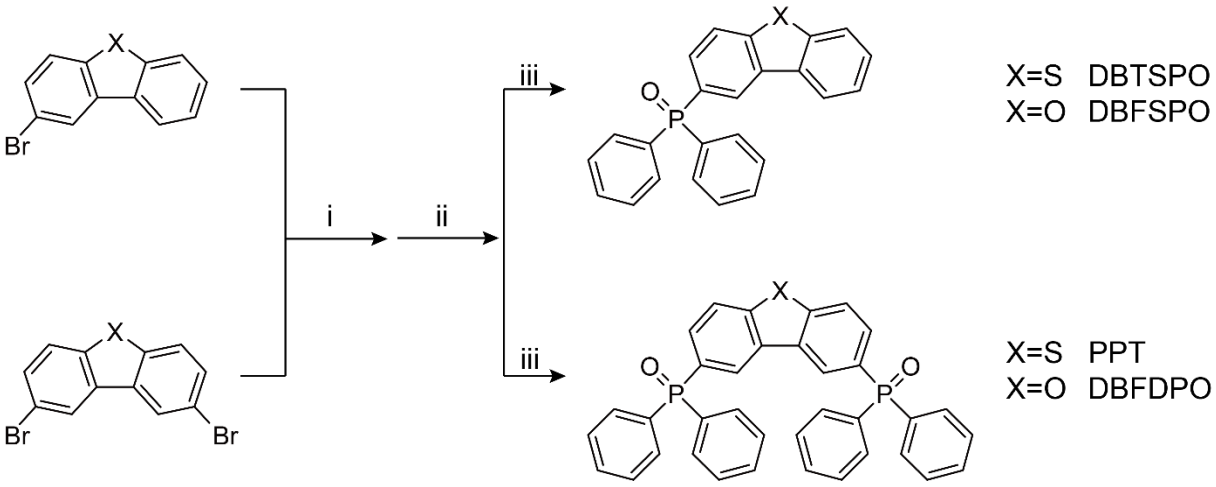


**Scheme S1**. Synthetic routes to DBTSPO, DBFSPO, PPT and DBFDPO. Reaction conditions: (i) *n*-BuLi, THF, -78ºC, 2 h; (ii) $Ph_2PCl$, -78ºC, 1 h; (iii) 30% $H_2O_2$ aqueous solution, $CH_2Cl_2$, room temperature (r.t.), overnight.

### Synthesis of dibenzo[b,d]thiophen-2-yldiphenylphosphine oxide (DBTSPO)

2-Bromodibenzo[b,d]thiophene (1.32 g, 5.00 mmol, 1.00 equivalent (eq.)) was dissolved in 30 mL anhydrous THF under Ar and cooled to -78ºC in a dry ice/acetone bath. *n*-BuLi (3.80 mL, 6.00 mmol, 1.20 eq., 1.60 M in hexane) was then added dropwise. Two hours later, diphenylphosphine chloride (1.20 mL, 6.50 mmol, 1.30 eq.) was injected into the system at -78°C and the mixture was stirred at this temperature for 1 h, following which the temperature was allowed to increase to r.t.. After stirred for 12 h, the reaction was quenched with 5 mL

water, then extracted by $CH_2Cl_2$ and washed by water. The organic layer was dried with anhydride $Na_2SO_4$ and the solvent was evaporated under reduced pressure. The resulting solid resides were dissolved in $CH_2Cl_2$ (20 mL) for oxidation by treating with 5 mL 30% $H_2O_2$ aqueous solution. After stirred overnight at r.t., the solvent was removed and the crude product was purified by a column chromatography using petrol ether and ethyl easter (3:1) as eluent to obtain a pure white solid. Yield: 0.81 g, 42%.$^1$H NMR (400 MHz, $CDCl_3$, ppm): δ = 8.61 (d, *J* = 12.6 Hz, 1H), 8.13 (d, *J* = 8.6 Hz, 1H), 7.90 (dd, *J* = 20.8, 8.4 Hz, 2H), 7.72 (dd, *J* = 12.6, 7.7 Hz, 4H), 7.58 (dd, *J* = 16.9, 9.2 Hz, 3H), 7.47 (dd, *J* = 14.3, 6.6 Hz, 6H). $^{13}$C NMR (101 MHz, $CDCl_3$, ppm): δ = 143.52, 143.49, 139.50, 135.73, 135.60, 134.79, 133.22, 132.21, 132.19, 132.12, 132.09, 129.31, 129.19, 128.73, 128.69, 128.57, 127.68, 127.51, 125.86, 125.76, 124.92, 122.97, 122.86, 122.84, 122.06. MALDI-TOF: m/z calcd for $C_{24}H_{17}OPS$ $[M]^+$: 384.430; Found: 384.904.

**Synthesis of dibenzo[b,d]furan-2-yldiphenylphosphine oxide (DBFSPO)**

DBFSPO was prepared under the identical synthetic conditions described in the preparation of DBTSPO using 2-bromodibenzo[b,d]furan (1.24 g, 5.00 mmol), *n*-BuLi (3.80 mL, 6.00 mmol, 1.20 eq., 1.60 M in hexane), diphenylphosphine chloride (1.20 mL, 6.50 mmol, 1.30 eq.) and 5 mL 30% $H_2O_2$ aqueous solution. Yield: 1.20 g, 65%. $^1$H NMR (400 MHz, $CDCl_3$, ppm): δ = 8.42 (d, *J* = 11.6 Hz, 1H), 7.92 (d, *J* = 7.4 Hz, 1H), 7.71 (dd, *J* = 12.0, 8.2 Hz, 4H), 7.64 (t, *J* = 11.3 Hz, 2H), 7.60–7.53 (m, 3H), 7.53–7.45 (m, 5H), 7.36 (t, *J* = 7.7 Hz, 1H). $^{13}$C NMR (101 MHz, $CDCl_3$, ppm): δ = 158.21, 158.18, 156.63, 133.18, 132.22, 132.12, 132.07, 131.68, 131.65, 131.34, 131.23, 130.91, 130.79, 128.68, 128.56, 128.32, 128.19, 128.10, 126.94, 125.88, 125.57, 125.46, 124.95, 124.80, 123.41, 123.32, 121.17, 112.04, 111.89. MALDI-TOF: m/z calcd for $C_{24}H_{17}O_2P$ $[M]^+$: 368.370; Found: 368.946.

**Synthesis of dibenzo[b,d]thiophene-2,8-diylbis(diphenylphosphine oxide) (PPT)**

PPT was prepared under the identical synthetic conditions described in the preparation of DBTSPO using 2,8-dibromodibenzo[b,d]thiophen (1.71 g, 5.00 mmol), *n*-BuLi (7.50 mL, 12.0 mmol, 2.40 eq., 1.60 M in hexane), diphenylphosphine chloride (2.30 mL, 13.0 mmol, 2.60 eq.) and 10 mL 30% $H_2O_2$ aqueous solution. Yield: 1.70 g, 58%. $^1$H NMR (400 MHz, $CDCl_3$, ppm): δ = 8.48 (d, *J* = 13.0 Hz, 2H), 7.97 (d, *J* = 8.2 Hz, 2H), 7.81–7.73 (m, 2H), 7.69 (dd, *J* = 12.1, 7.0 Hz, 8H), 7.57 (t, *J* = 7.4 Hz, 4H), 7.48 (t, *J* = 7.4 Hz, 8H). $^{13}$C NMR (101 MHz, $CDCl_3$, ppm): δ = 143.57, 143.55, 134.94, 134.81, 132.82, 132.23, 132.21, 132.13,

132.03, 131.78, 130.20, 130.09, 129.53, 128.76, 128.64, 128.49, 126.01, 125.91, 123.18, 123.05. MALDI-TOF: m/z calcd for $C_{36}H_{26}O_2P_2S$ $[M]^+$: 584.610; Found: 584.498.

**Synthesis of dibenzo[b,d]furan-2,8-diylbis(diphenylphosphine oxide) (DBFDPO)**

DBFDPO was prepared under the identical synthetic conditions described in the preparation of DBTSPO using 2,8-dibromodibenzo[b,d]furan (1.63 g, 5.00 mmol), *n*-BuLi (7.50 mL, 12.0 mmol, 2.40 eq., 1.60 M in hexane), diphenylphosphine chloride (2.30 mL, 13.0 mmol, 2.60 eq.) and 10 mL 30% $H_2O_2$ aqueous solution. Yield: 2.16 g, 76%. $^1$H NMR (400 MHz, $CDCl_3$, ppm): δ = 8.28 (d, *J* = 11.7 Hz, 2H), 7.84–7.75 (m, 2H), 7.68 (dd, *J* = 12.0, 8.1 Hz, 10H), 7.57 (t, *J* = 7.5 Hz, 4H), 7.48 (t, *J* = 7.9 Hz, 8H). $^{13}$C NMR (101 MHz, $CDCl_3$, ppm): δ = 158.55, 158.52, 132.91, 132.21, 132.19, 132.09, 131.99, 131.87, 131.75, 131.64, 128.74, 128.62, 128.11, 127.06, 125.81, 125.70, 123.94, 123.79, 112.39, 112.26. MALDI-TOF: m/z calcd for $C_{36}H_{26}O_3P_2$ $[M]^+$: 568.550; Found: 568.746.

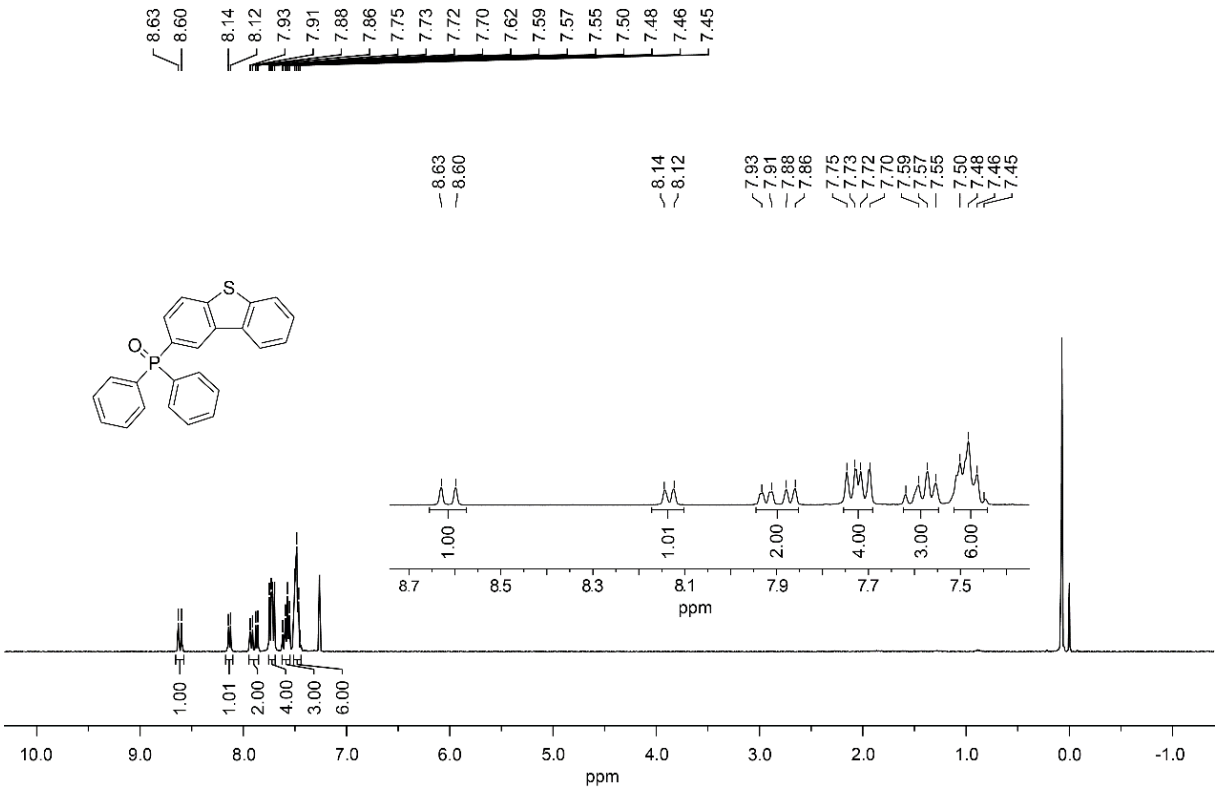


**Figure S1.** $^1$H NMR spectrum of DBTSPO in $CDCl_3$.

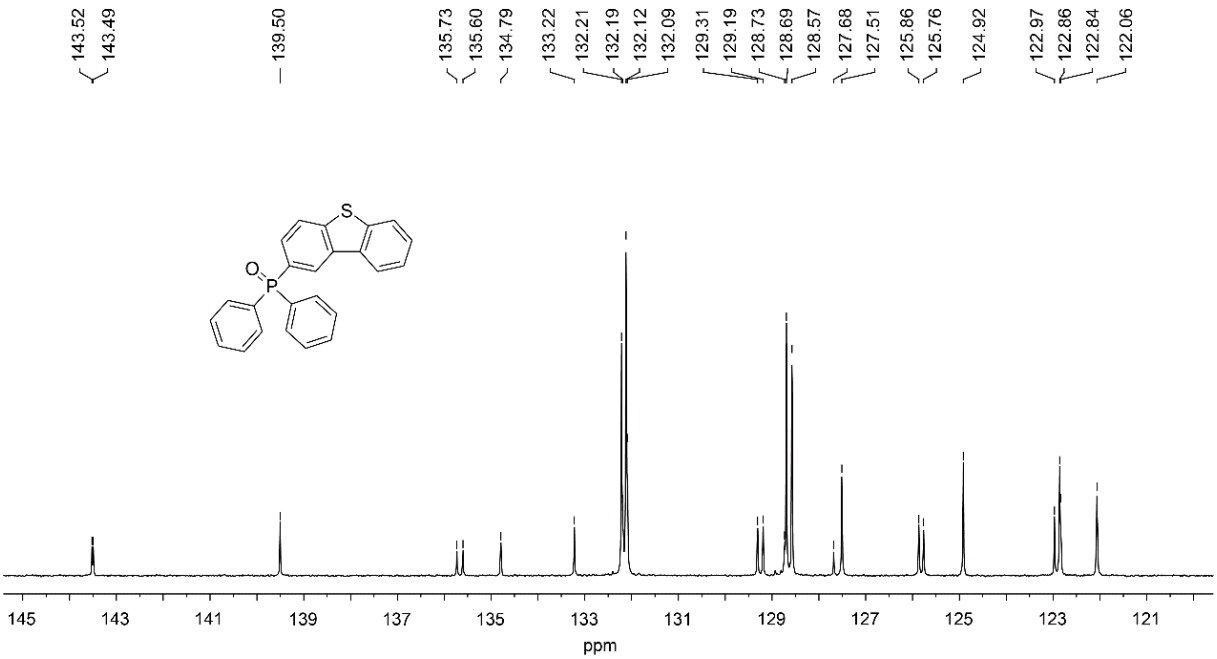


**Figure S2.** $^{13}C$ NMR spectrum of DBTSPO in $CDCl_3$.

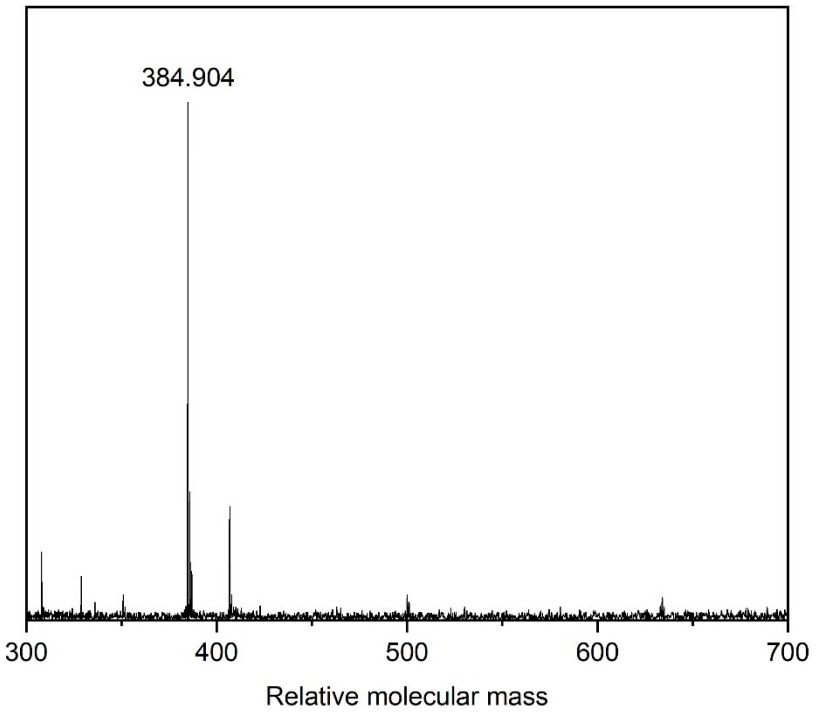


**Figure S3.** MALDI-TOF spectrum of DBTSPO.

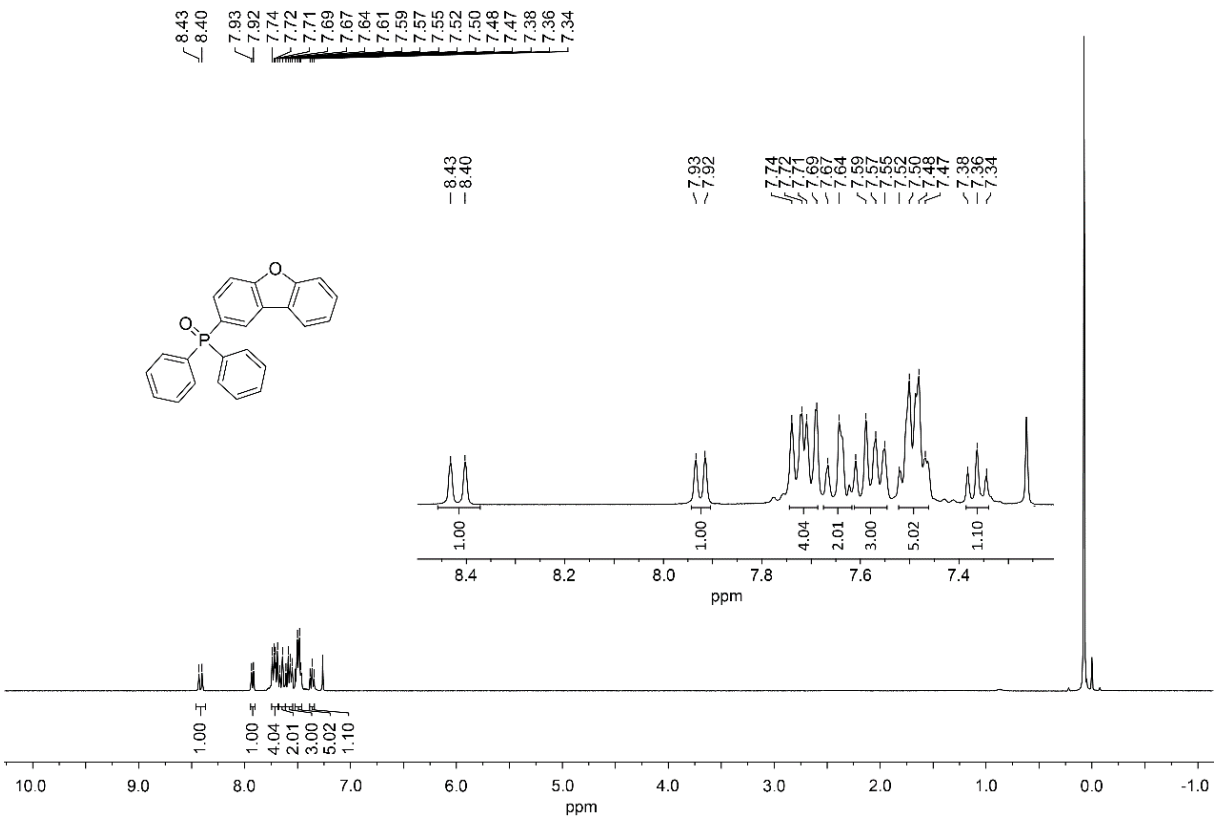


**Figure S4.** $^{1}$H NMR spectrum of DBFSPO in $CDCl_3$.

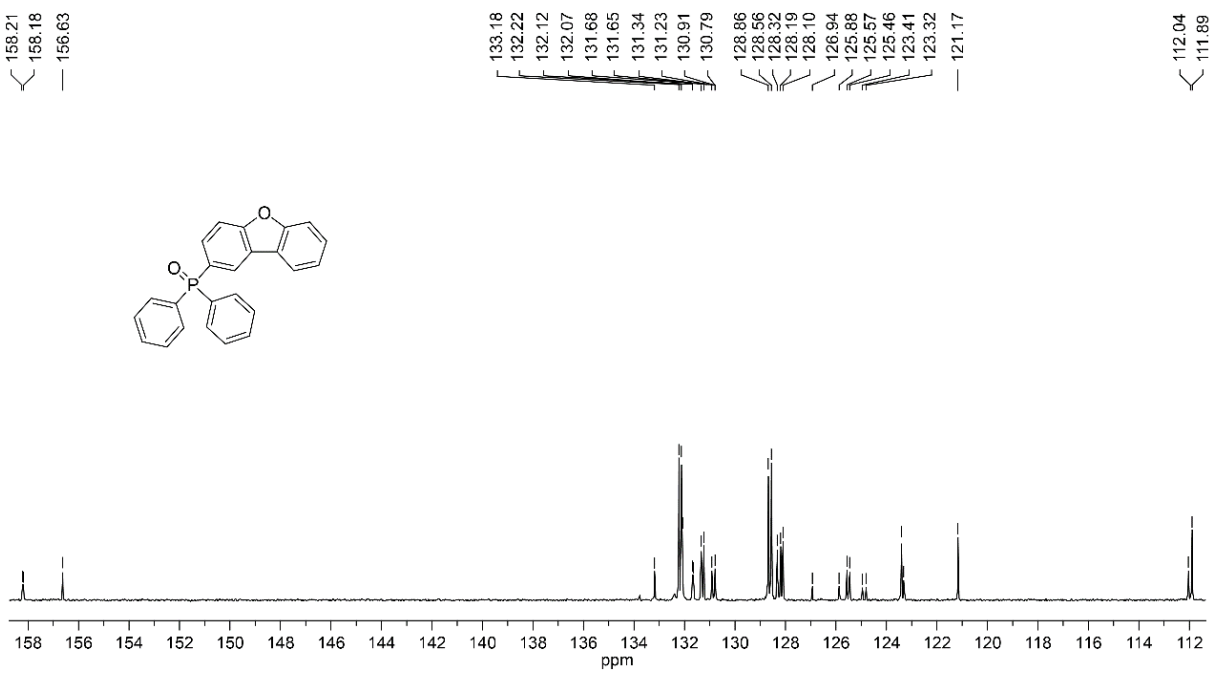


**Figure S5.** $^{13}$C NMR spectrum of DBFSPO in $CDCl_3$.

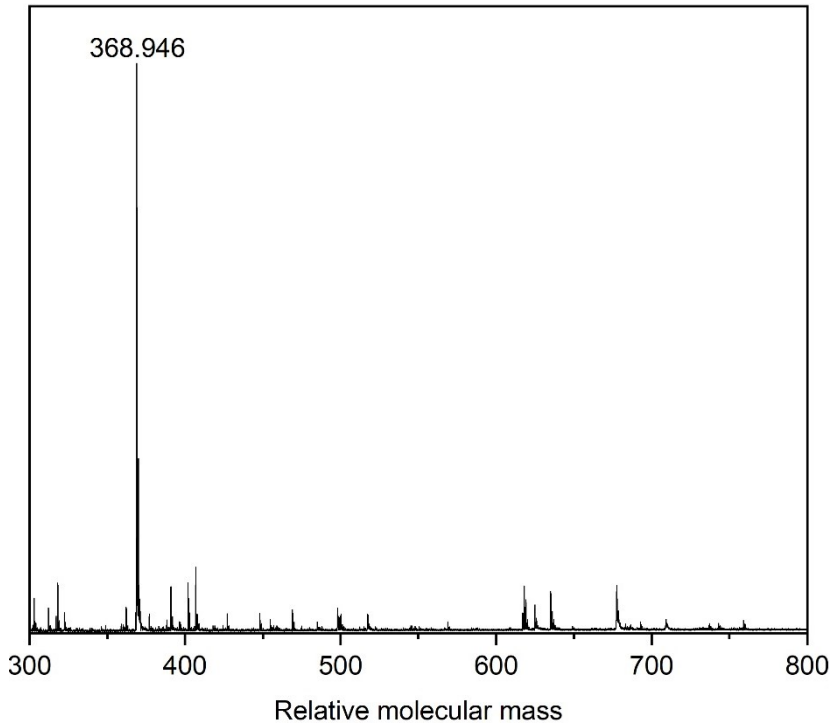


**Figure S6.** MALDI-TOF spectrum of DBFSPO.

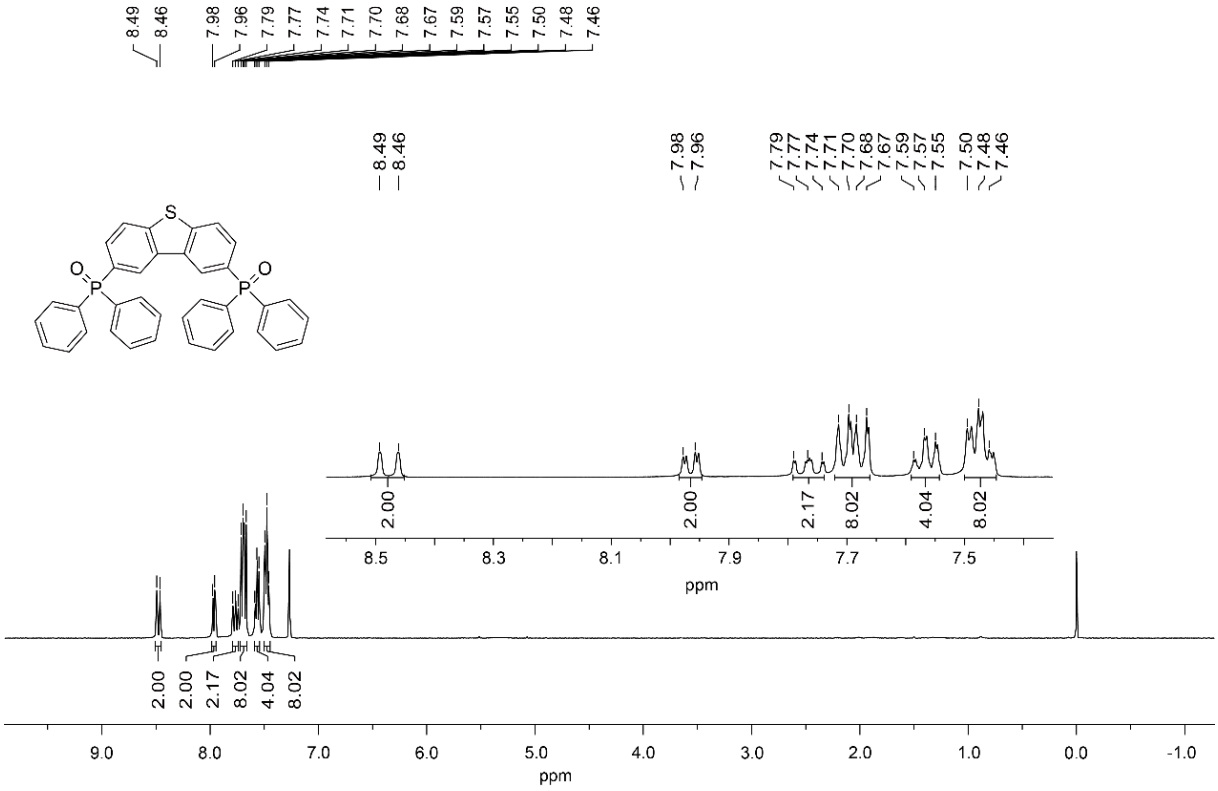


**Figure S7.** $^{1}H$ NMR spectrum of PPT in $CDCl_3$.

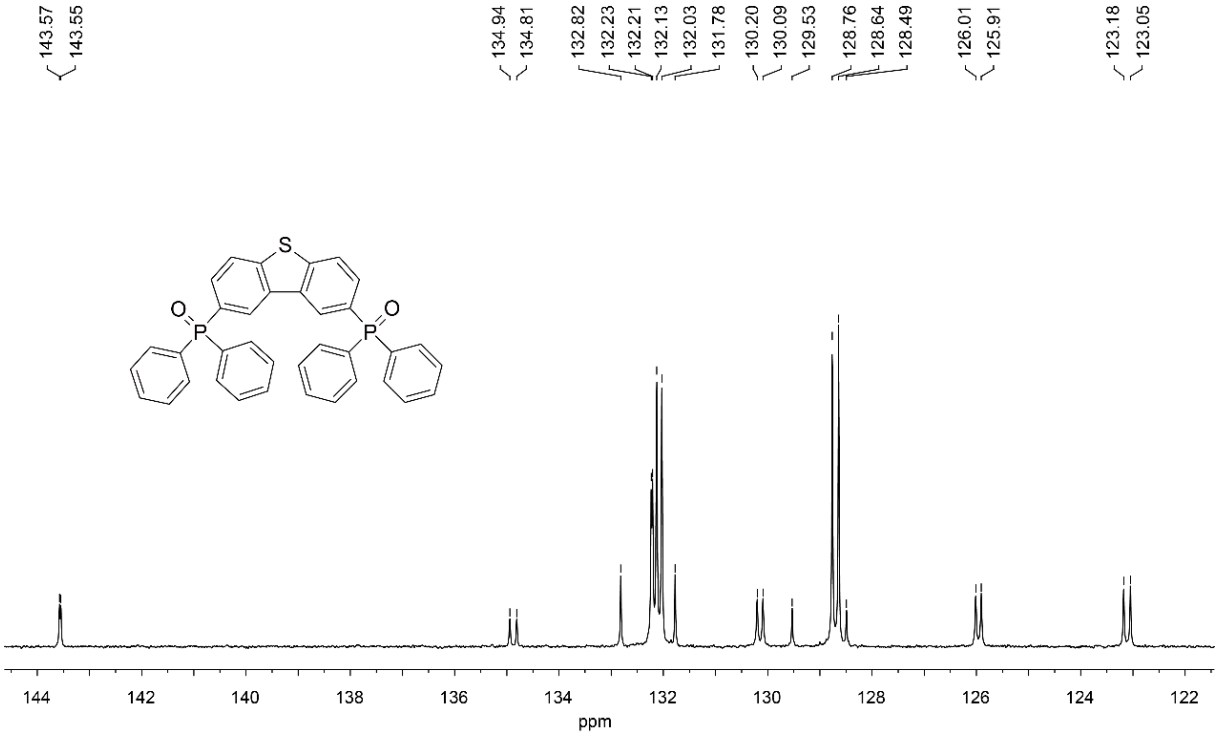


**Figure S8.** $^{13}C$ NMR spectrum of PPT in $CDCl_3$.

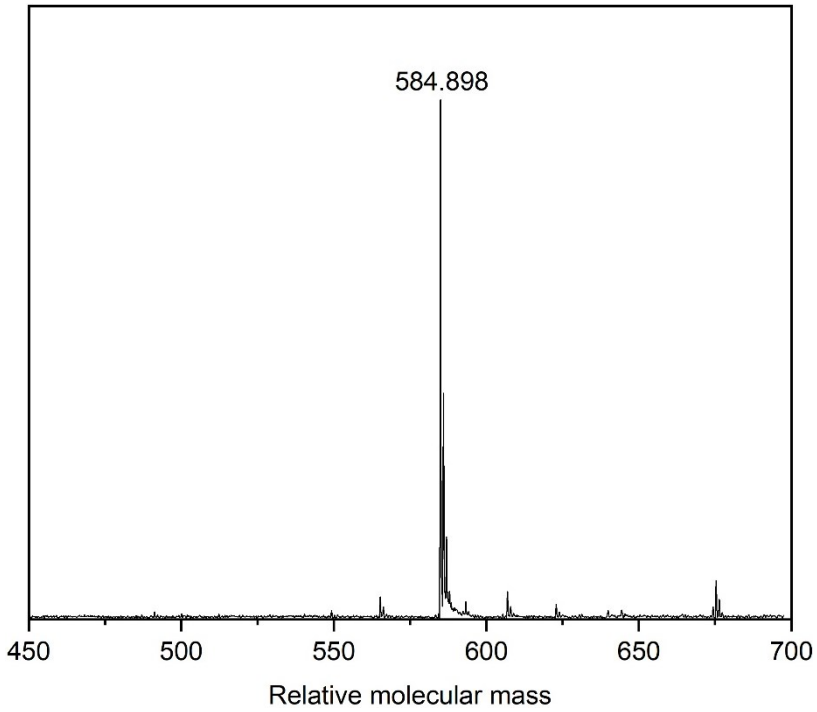


**Figure S9.** MALDI-TOF spectrum of PPT.

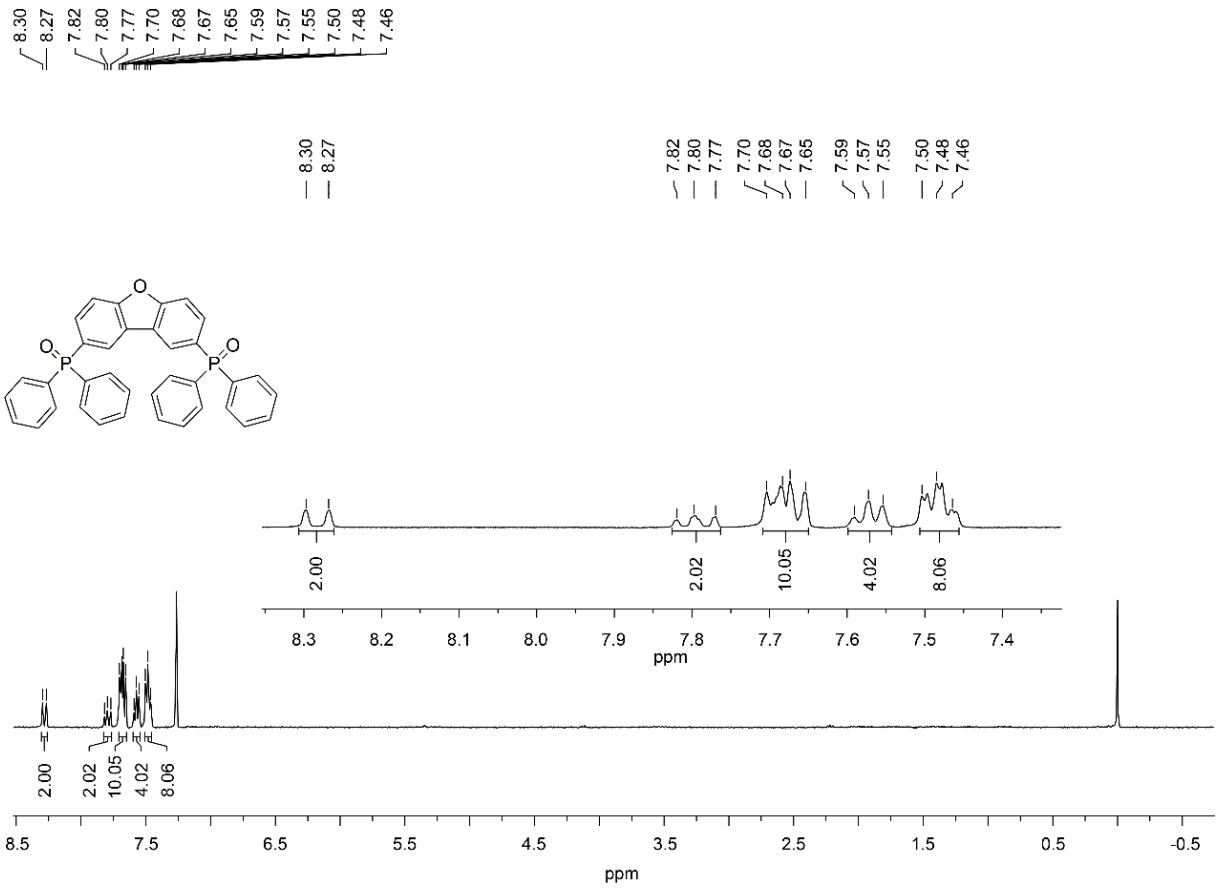


**Figure S10.** $^{1}$H NMR spectrum of DBFDPO in $CDCl_3$.

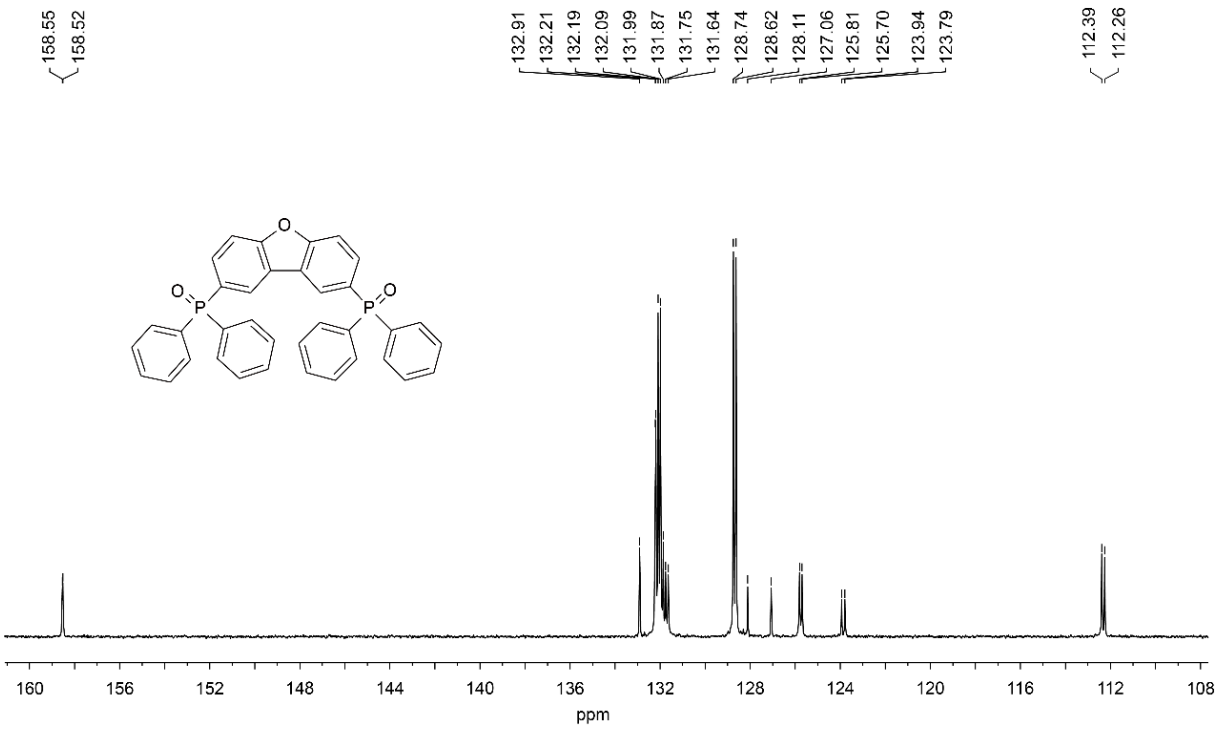


**Figure S11.** $^{13}$C NMR spectrum of DBFDPO in $CDCl_3$.

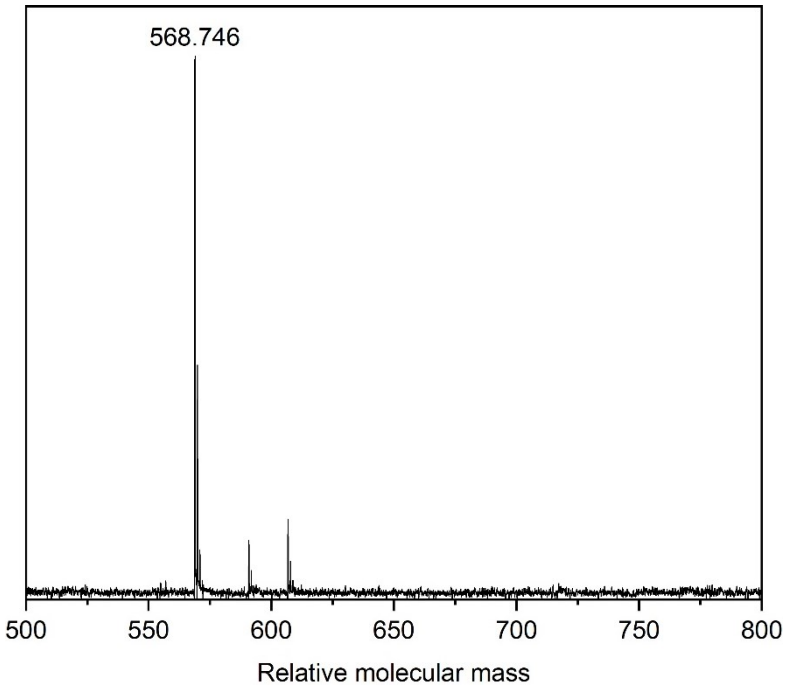


**Figure S12.** MALDI-TOF spectrum of DBFDPO.

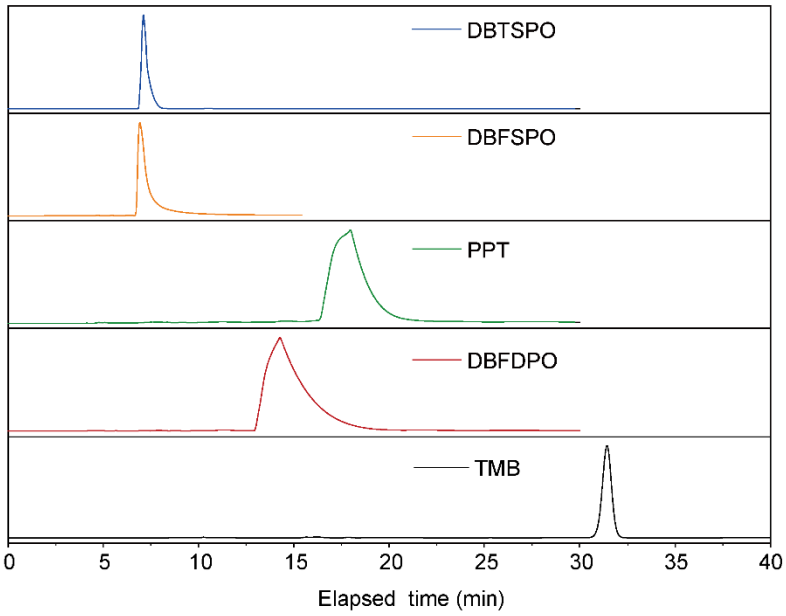


**Figure S13.** HPLC spectra of DBTSPO, DBFSPO, PPT, DBFDPO and TMB.

## 2. Thermal properties

Thermogravimetric analyses (TGA) were conducted on a DTG-60 Shimadzu thermal analyst system under a heating rate of 10ºC/min and a nitrogen flow rate of 50 $cm^3$/min. The differential scanning calorimetry (DSC) analyses were performed on a Shimadzu DSC-60A instrument under a heating rate of 10ºC/min and a nitrogen flow rate of 20 $cm^3$/min.

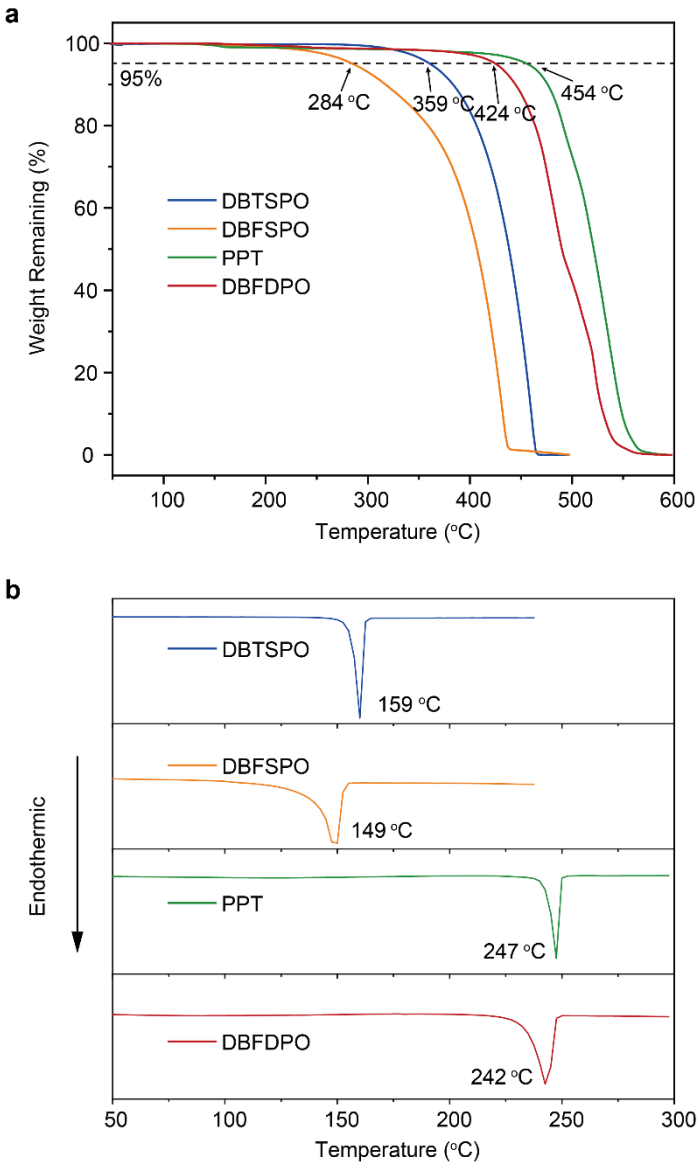


**Figure S14.** TGA (a) and DSC (b) curves of DBTSPO, DBFSPO, PPT and DBFDPO.

## 3. Electrochemical properties

Cyclic voltammogram (CV) measurements were performed at r.t. on a CHI660E system in a typical three-electrode cell with a working electrode (glass carbon), a reference electrode ($Ag/Ag^+$, referenced against ferrocene/ferrocenium (FOC)), and a counter electrode (Pt wire) in an acetonitrile solution of tetrabutylammonium hexafluorophosphate ($Bu_4NPF_6$) (0.1 M) at a sweeping rate of 100 mV $s^{-1}$. HOMO energy levels ($E_{HOMO}$) of the host materials were estimated based on the reference energy level of ferrocene (4.8 eV below the vacuum) according to the Equations S1:

$$E_{HOMO} = -\left\lfloor E_{onset}^{Ox} - (0.04) \right\rfloor - 4.8 \text{ eV} \quad \text{.....S1}$$

where the value of 0.04 V is the onset oxidative voltage of FOC *vs* $Ag/Ag^+$ and $E_{onset}^{Ox}$ is the onset potential of the oxidation. The calibrated oxidation potential of FOC was calculated to be 0.04 eV. LUMO energy level ($E_{LUMO}$) was estimated by adding the optical band-gap ($E_g$) to the corresponding HOMO energy level as in Equations S2.

$$E_{LUMO} = (E_g + E_{HOMO})\,\text{eV} \quad \text{.....S2}$$

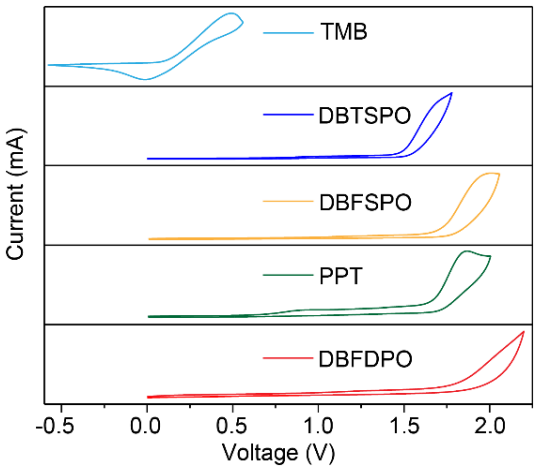


**Figure S15.** CV curves of TMB, DBTSPO, DBFSPO, PPT and DBFDPO.

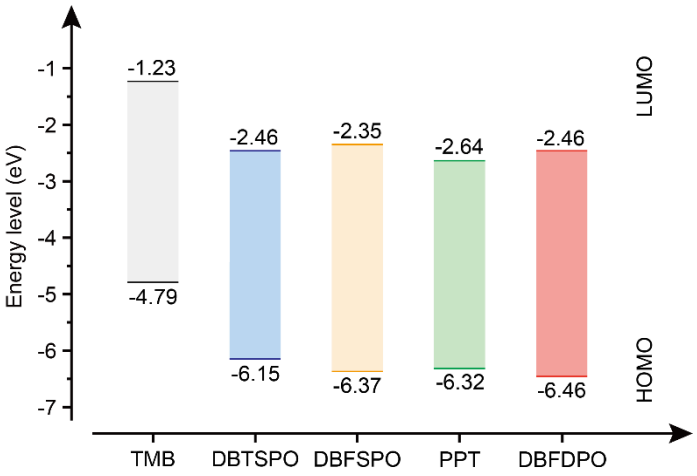


**Figure S16.** HOMO and LUMO energy levels of TMB, DBTSPO, DBFSPO, PPT and DBFDPO.

## 4. Morphology characterization

Powder X-ray diffraction (XRD) patterns were measured using a Bruker D8 Advance diffractometer (Cu Kα: λ = 1.5418 Å) under ambient conditions.

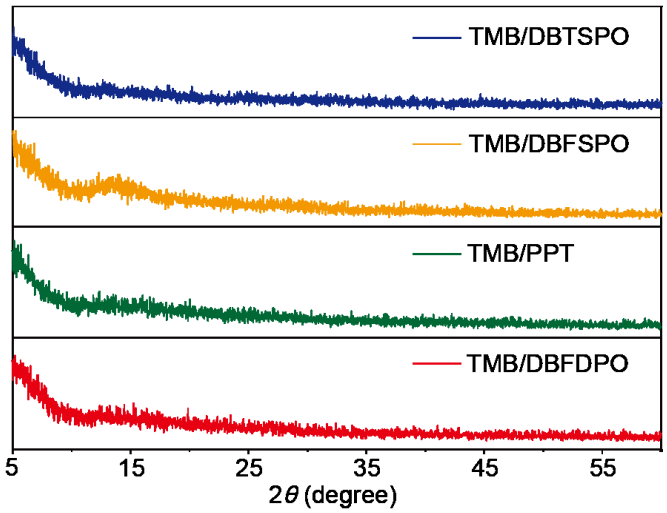


**Figure S17.** Powder-XRD patterns of 1 mol% TMB/acceptor doped films.

## 5. Photophysical properties and ESR measurements

Ultraviolet/visible (UV/Vis) and fluorescence spectra were recorded on V-750 spectrophotometer and Edinburgh FLS980, respectively. The absolute photoluminescence quantum yield (PLQY) was obtained using an Edinburgh FLS980 fluorescence spectrophotometer equipped with an integrating sphere. Phosphorescence spectra were obtained using an Edinburgh FLS980 fluorescence spectrophotometer with a 10 ms delay time after excitation using a microsecond flash lamp. The microsecond flash lamp produces short, typically a few μs, and high irradiance optical pulses for phosphorescence decay measurements in the range from microseconds to seconds. For fluorescence decay measurements, picosecond pulsed light-emitting diodes (EPLED-380, wavelength: 377 nm, pulse width: 947.7 ps; EPLED-295, wavelength: 300 nm, pulse width: 833.7 ps) were used. Electron spin resonance (ESR) spectra were recorded on a Bruker microESR MS 5000 spectrometer. The samples for ESR measurement were prepared by adding the donor/acceptor mixtures into a quartz ESR tube followed by heating them up to melt in a glove box.

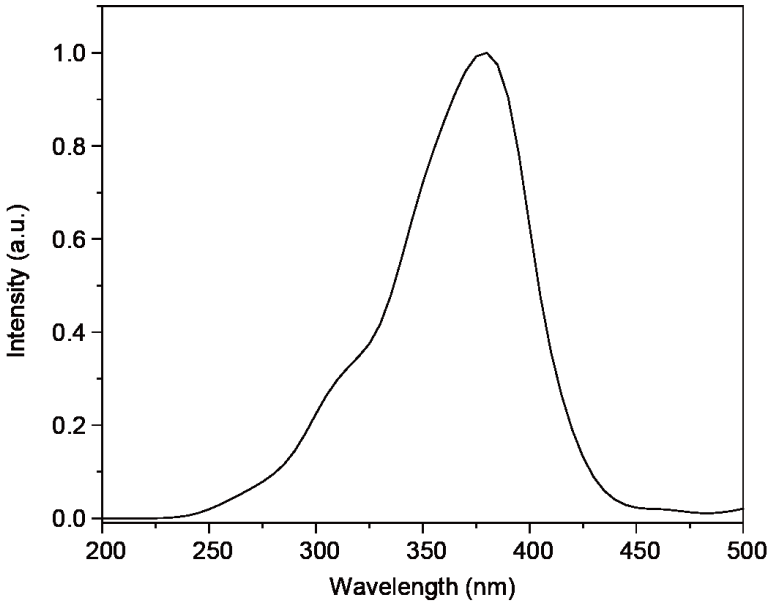


**Figure S18.** Normalized excitation spectrum of 1 mol% TMB/DBTSPO doped film at 512 nm.

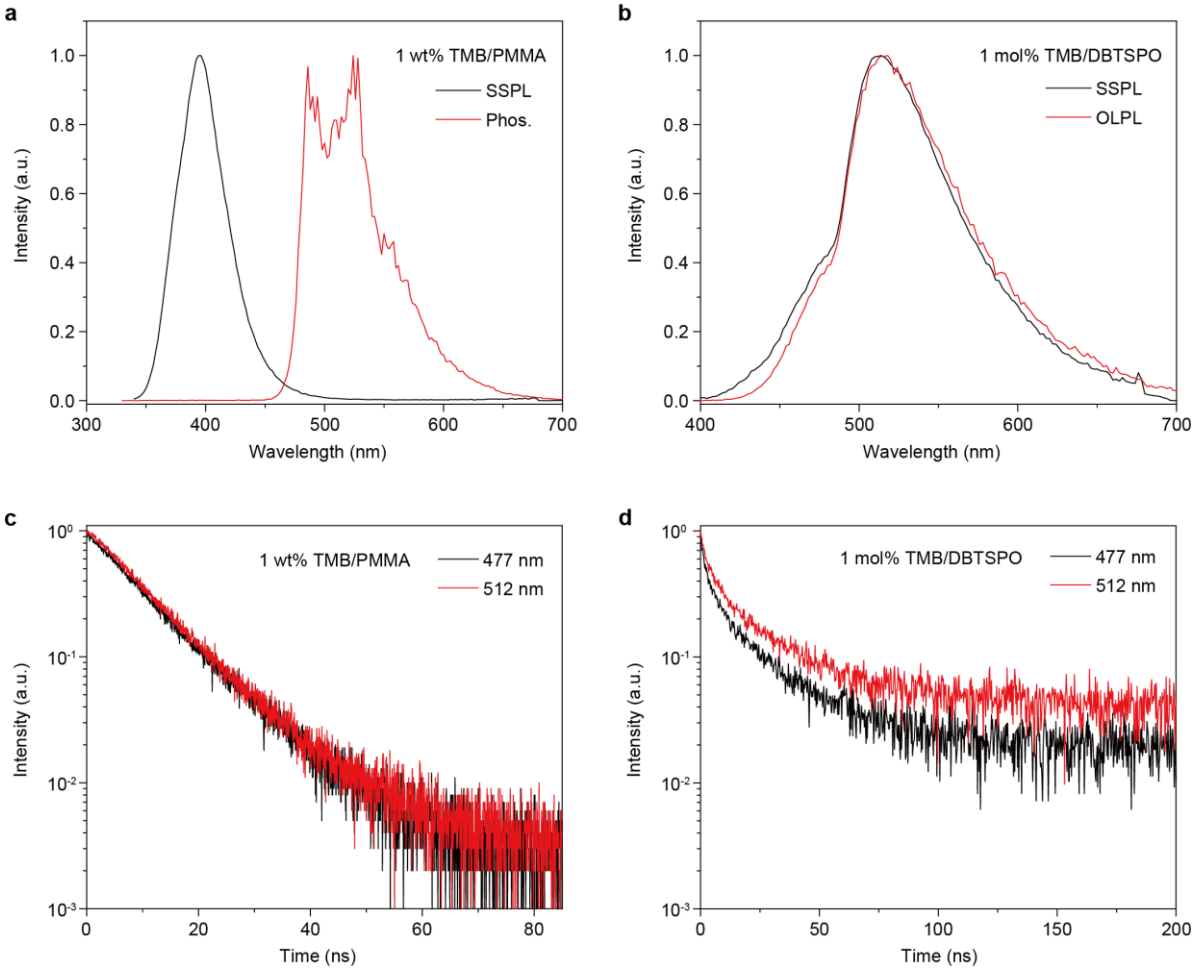


**Figure S19.** (a, b) Steady-state photoluminescence (SSPL) and phosphorescence spectra of (a) 1 wt% TMB/PMMA and (b) 1 mol% TMB/DBTSPO doped films. (c, d) Transient photoluminescence decay profiles of (c) 1 wt% TMB/PMMA and (d) 1 mol% TMB/DBTSPO doped films monitored at 477 and 512 nm respectively.

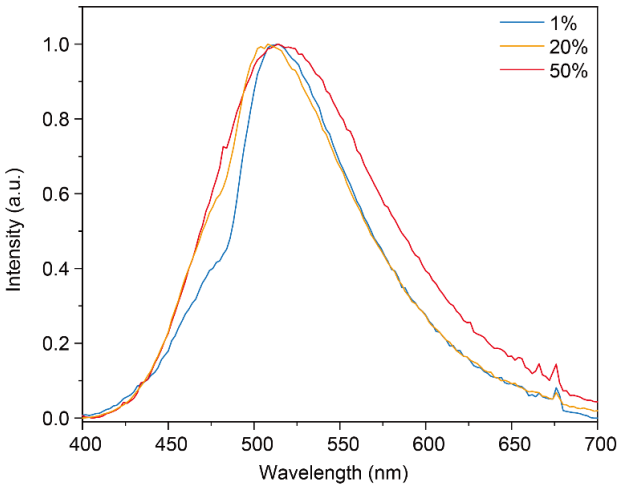


**Figure S20.** Normalized steady-state photoluminescence (SSPL) spectra of 1 mol% TMB/DBTSPO at different doping concentrations.

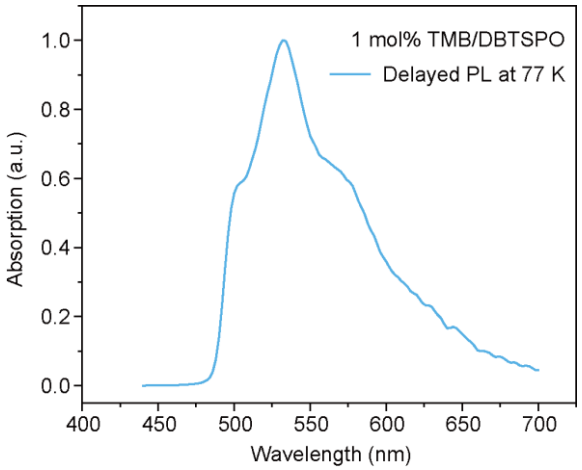


**Figure S21**. Delayed photoluminescence (PL) of 1 mol% TMB/DBTSPO film at 77 K (a delay time of 10 ms). The excitation wavelength is 385 nm.

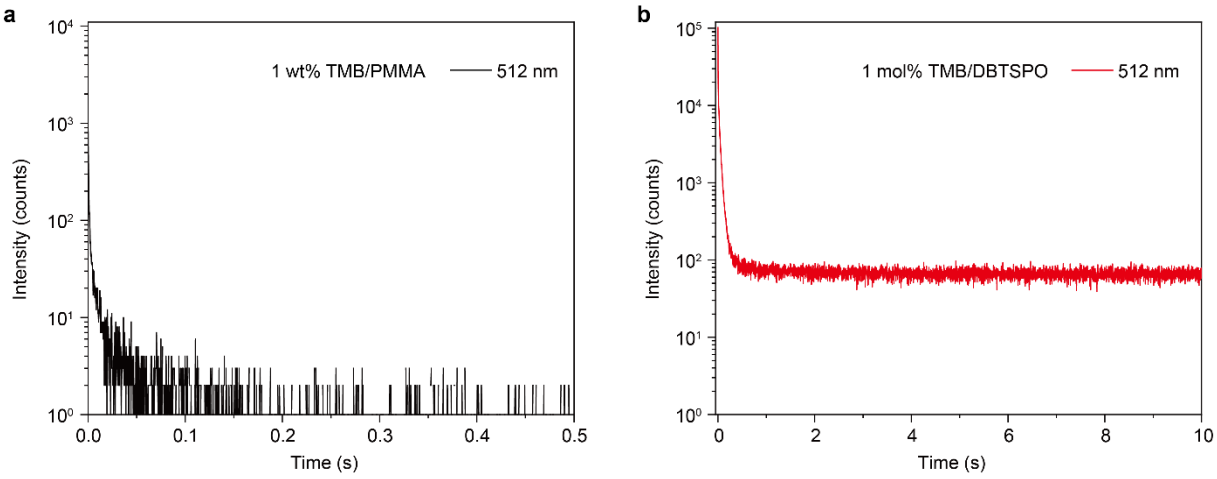


**Figure S22.** Phosphorescence lifetime decay profiles of (a) 1 wt% TMB/PMMA and (b) 1 mol% TMB/DBTSPO doped films monitored at 512 nm.

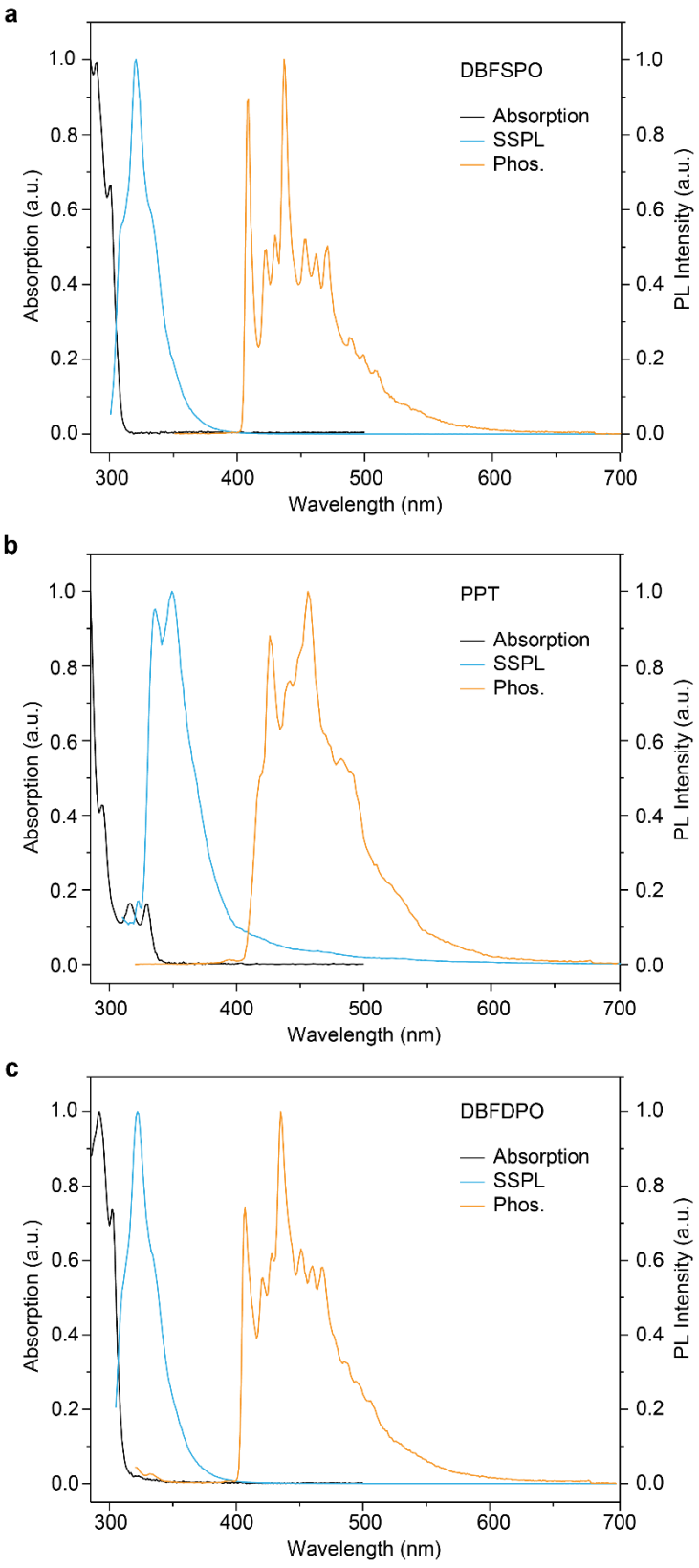


**Figure S23.** UV-vis absorption, SSPL and phosphorescence spectra of (a) DBFSPO, (b) PPT, (c) DBFDPO measured in toluene solution at a concentration of $10^{-5}$ mol/L. The absorption and SSPL spectra were tested at r.t., while phosphorescence spectra were measured at 77 K.

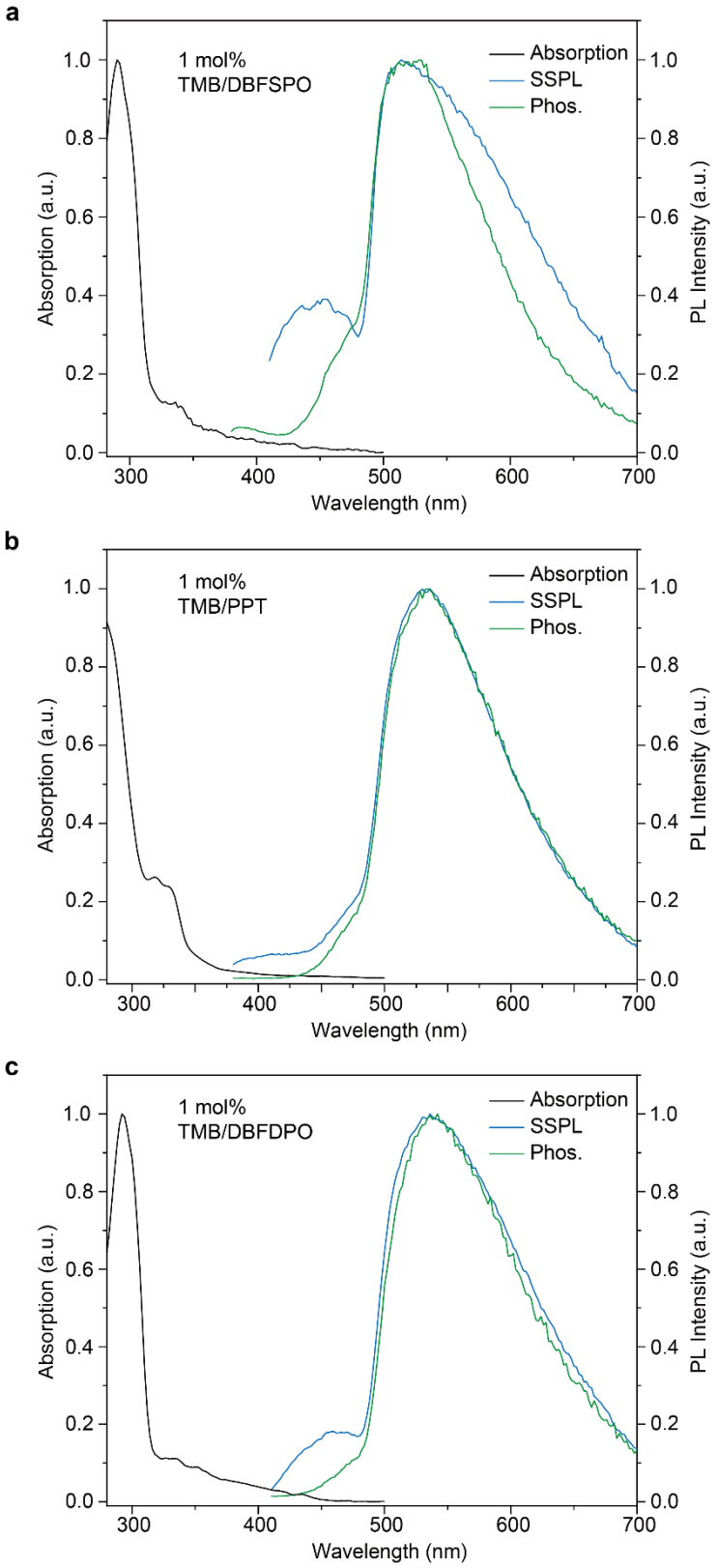


**Figure S24.** UV-vis absorption, SSPL and phosphorescence spectra of (a) TMB/DBFSPO, (b) TMB/PPT and (c) TMB/DBFDPO doped films.

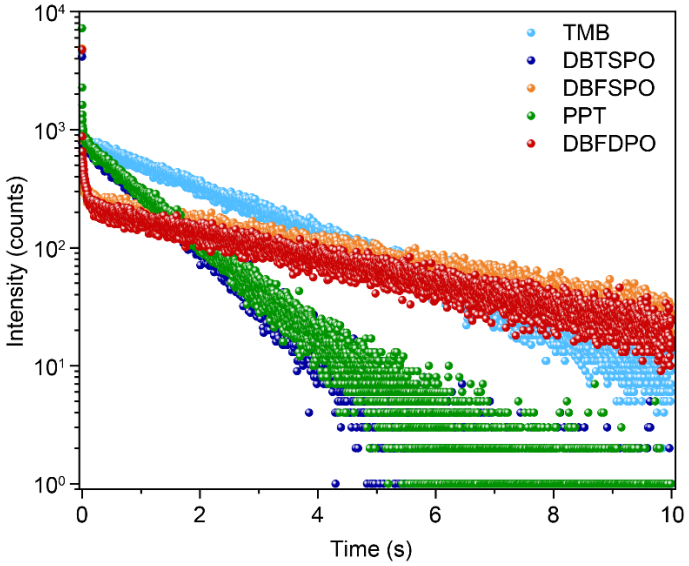


**Figure S25.** Lifetime decay profiles of TMB, DBTSPO, DBFSPO, PPT and DBFDPO at 519, 427, 436, 456 and 435 nm respectively measured at 77 K in toluene.

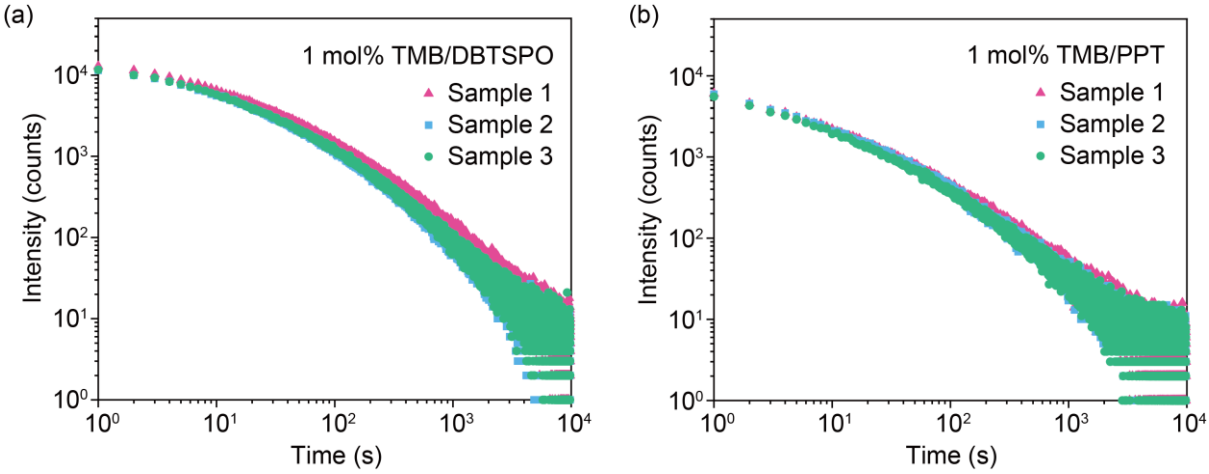


**Figure S26**. Logarithmic plot of the emission decay profiles of 1 mol% TMB/DBTSPO (a) and 1 mol% TMB/PPT (b) films (excitation time: 200 s; power density: 4.2 mW/cm$^2$).

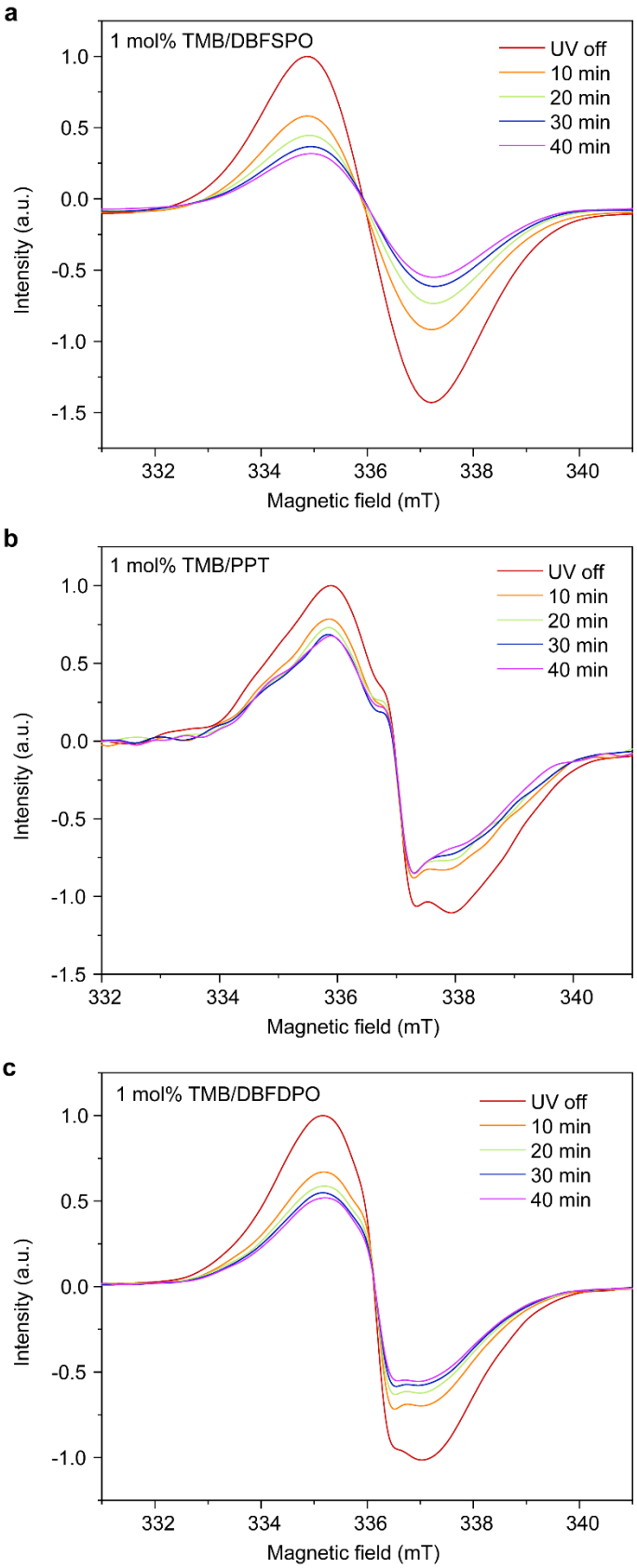


**Figure S27.** Time-dependent ESR spectra of (a) TMB/DBFSPO, (b) TMB/PPT, and (c) TMB/DBFDPO doped films after turning off 365 nm UV light. The excitation duration of UV light is 60 s.

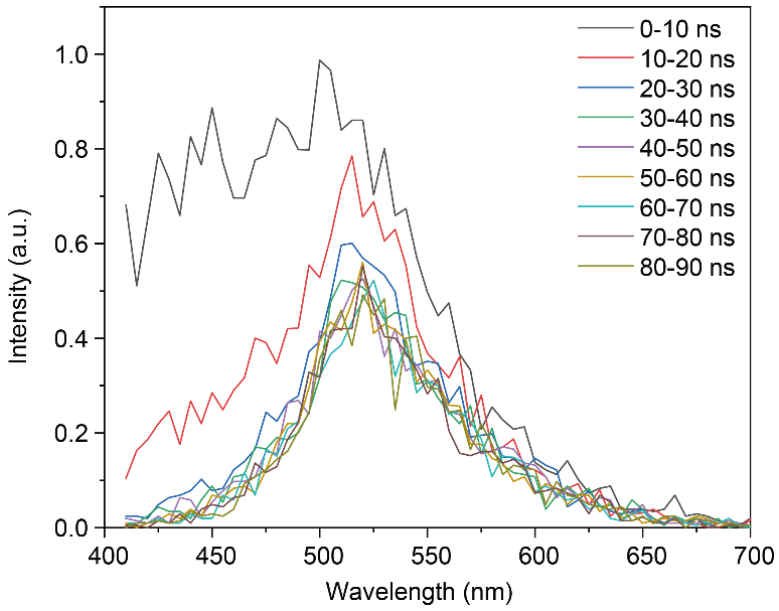


**Figure S28.** Time-resolved photoluminescence spectra of 1 mol% TMB/DBTSPO doped film.

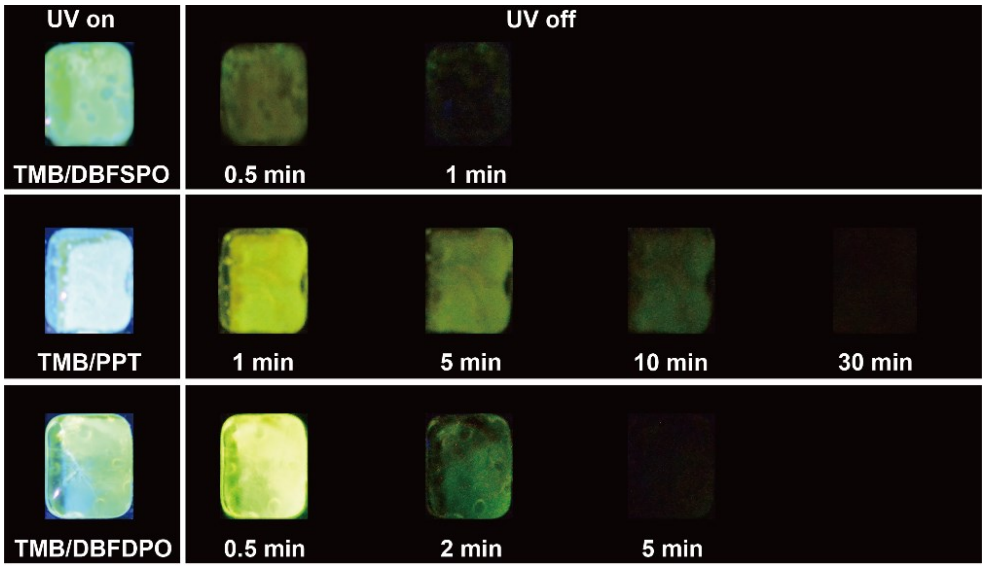


**Figure S29.** Photographs of 1 mol% TMB/acceptor doped films taken under and after the removal of 385 nm excitation source (excitation time: 60 s; power density: 1.3 W/cm$^2$).

## 6. Variable temperature kinetics lifetimes and photoluminescence spectra

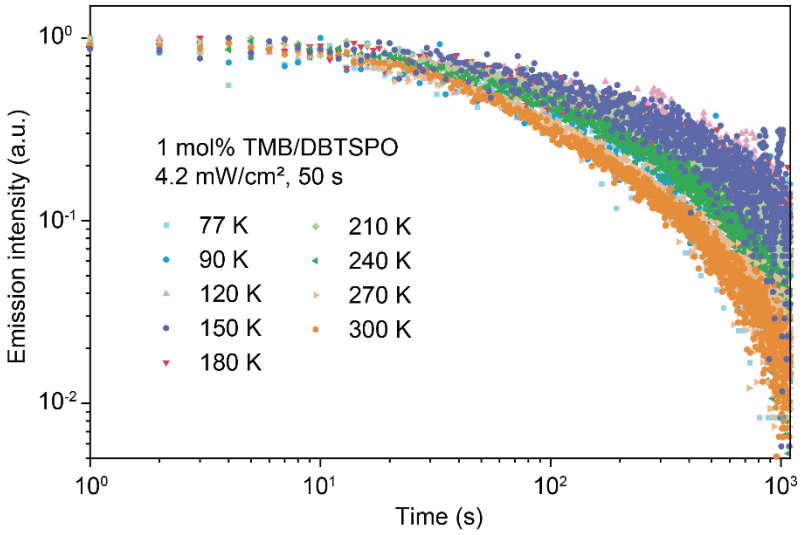


**Figure S30**. OLPL decay profiles for 1 mol% TMB/DBTSPO doped films under different temperatures (power density: 4.2 mW/cm$^2$; excitation time: 50 s).

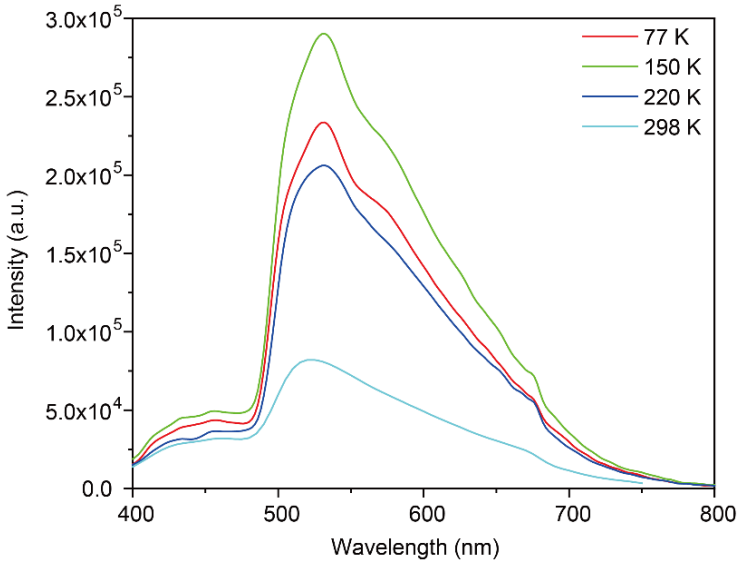


**Figure S31.** SSPL spectra of 1 mol% TMB/DBTSPO doped film at different temperatures (77-298 K).

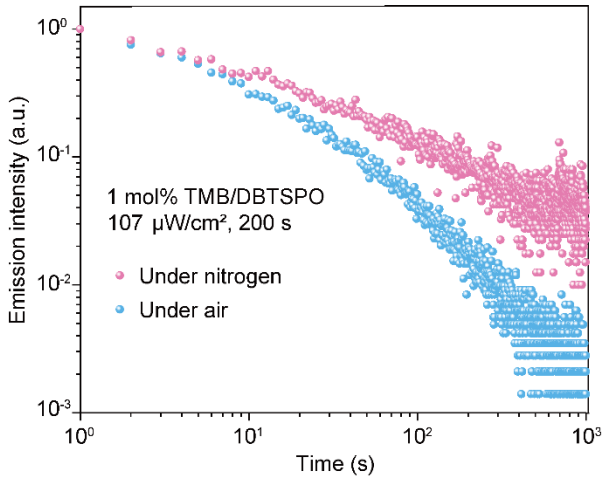


**Figure S32**. Logarithmic plot of the emission decay profiles of 1 mol% TMB/DBTSPO doped film under nitrogen (pink) and under air (blue) conditions. (excitation time: 200 s; power density: 107 μW/cm$^2$).

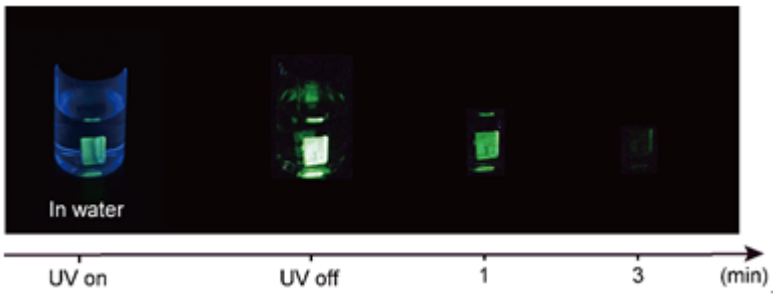


**Figure S33**. Photographs of 1 mol% TMB/DBTSPO doped film without encapsulation in water taken under and after the removal of 385 nm excitation source (excitation time: 10 s; power density: 1.3 W/cm$^2$)

## 7. Excited state energy and natural transition orbit calculations

The energies of the lowest singlet excited state ($S_1$) and triplet excited state ($T_1$) were computed by the functional of B3LYP/6-31g(d) based on the optimized ground state structure. In order to better describe the transition properties of excited states, natural transition orbits (NTO) are analyzed based on $S_0$ state optimization configuration.

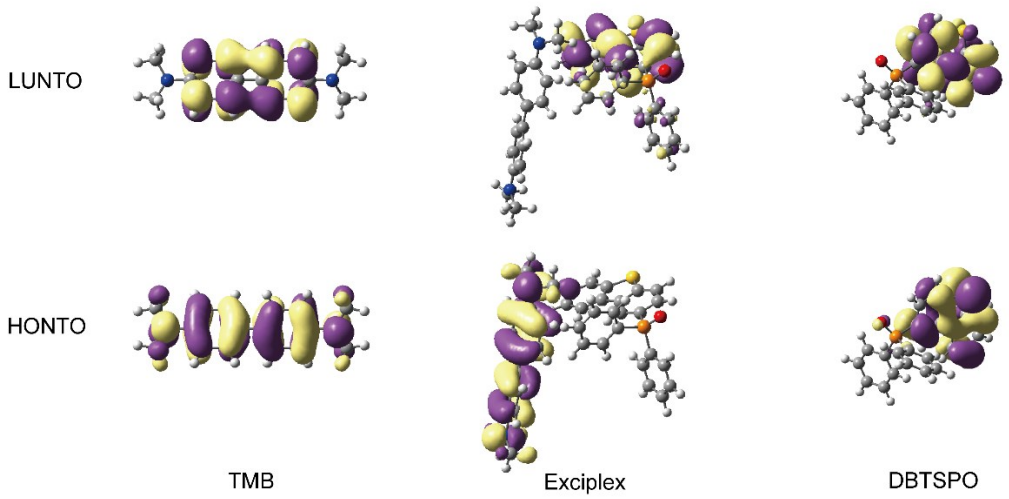


**Figure S34**. Lowest unoccupied NTO (LUNTO) and highest occupied NTO (HONTO) distributions of TMB, DBTSPO and their exciplex.

**Table S1.** Calculated $S_1$ and $T_1$ energy levels of TMB, DBTSPO and their exciplex.

| Energy level | TMB | DBTSPO | Exciplex |
|---|---|---|---|
| $S_1$ (eV) | 4.1932 | 4.1743 | 3.1192 |
| $T_1$ (eV) | 2.9971 | 3.1454 | 2.9757 |

## 8. Fabrication procedure of afterglow LED bulb

The preparation procedure of afterglow LED bulb is shown as follows. Firstly, the 1 mol% TMB and DBTSPO mixture was heated to a molten state in the glove box for 1 min. Then, the molten mixture was quickly transferred onto a lampshade. After the mixture was quickly cooled to room temperature, the lampshade was encapsulated by a layer of ultraviolet curing agent. Then, the prepared lampshade is placed on a 365 nm UV-chip, which can be lit by electro-excitation to achieve OLPL lighting.

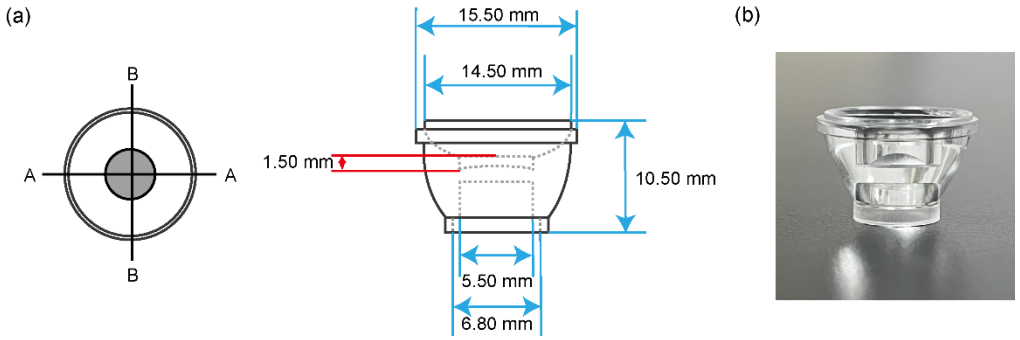


**Figure S35.** Design drawing (a) and photo (b) of the lampshade used in the smart lighting device.

**Table S2.** Code for time controller in afterglow lighting device. The power-on and -off durations are set to 60 and 300 s respectively.

```
void setup() {
pinMode(9, OUTPUT);
}
void loop() {
digitalWrite(9, HIGH);
delay(60000);
digitalWrite(9, LOW);
delay(300000);
}
```